RBF interpolation of boundary values in the BEM for heat transfer problems

Nam Mai-Duy and Thanh Tran-Cong
Faculty of Engineering and Surveying, University of Southern Queensland, Toowoomba, Australia

Received February 2002
Revised September 2002
Accepted January 2003

Keywords *Boundary element method, Boundary integral equation, Heat transfer*

Abstract *This paper is concerned with the application of radial basis function networks (RBFNs) as interpolation functions for all boundary values in the boundary element method (BEM) for the numerical solution of heat transfer problems. The quality of the estimate of boundary integrals is greatly affected by the type of functions used to interpolate the temperature, its normal derivative and the geometry along the boundary from the nodal values. In this paper, instead of conventional Lagrange polynomials, interpolation functions representing these variables are based on the "universal approximator" RBFNs, resulting in much better estimates. The proposed method is verified on problems with different variations of temperature on the boundary from linear level to higher orders. Numerical results obtained show that the BEM with indirect RBFN (IRBFN) interpolation performs much better than the one with linear or quadratic elements in terms of accuracy and convergence rate. For example, for the solution of Laplace's equation in 2D, the BEM can achieve the norm of error of the boundary solution of $O(10^{-5})$ by using IRBFN interpolation while quadratic BEM can achieve a norm only of $O(10^{-2})$ with the same boundary points employed. The IRBFN-BEM also appears to have achieved a higher efficiency. Furthermore, the convergence rates are of $O(h^{1.38})$ and $O(h^{4.78})$ for the quadratic BEM and the IRBFN-based BEM, respectively, where h is the nodal spacing.*

1. Introduction

Boundary element methods (BEMs) have become one of the popular techniques for solving boundary value problems in continuum mechanics. For linear homogeneous problems, the solution procedure of BEM consists of two main stages:

(1) estimate the boundary solution by solving boundary integral equations (BIEs), and

(2) estimate the internal solution by calculating the boundary integrals (BIs) using the results obtained from the stage (1).

Invited paper for the special issue of the *International Journal of Numerical Methods for Heat & Fluid Flow* on the BEM.

This work is supported by a Special USQ Research Grant (Grant No. 179-310) to Thanh Tran-Cong. This support is gratefully acknowledged. The authors would like to thank the referees for their helpful comments.

International Journal of Numerical Methods for Heat & Fluid Flow
Vol. 13 No. 5, 2003
pp. 611-632

0961-5539
DOI 10.1108/09615530310482472

The first stage plays an important role, because the solution obtained here provides sources to compute the internal solution. However, it can be seen that both stages involve the evaluation of BIs, of which any improvements achieved result in the betterment of the overall solution to the problem. In the evaluation of BIs, the two main topics of interest are how to represent the variables along the boundary adequately and how to evaluate the integrals accurately, especially in the cases where the moving field point coincides with the source point (singular integrals). In the standard BEM (Banerjee and Butterfield, 1981; Brebbia *et al.*, 1984), the boundary of the domain of analysis is divided into a number of small segments (elements). The geometry of an element and the variation of temperature and temperature gradient over such an element are usually represented by Lagrange polynomials, of which the constant, linear and quadratic types are the most widely applied. With regard to the evaluation of integrals, including weakly and strongly singular integrals, considerable achievements have been reported by Sladek and Sladek (1998). It is observed that the accuracy of solution by the standard BEM greatly depends on the type of elements used. On the other hand, neural networks (NN) which deal with interpolation and approximation of functions, have been developed recently and become one of the main fields of research in numerical analysis (Haykin, 1999). It has been proved that the NNs are capable of universal approximation (Cybenko, 1989; Girosi and Poggio, 1990). Interest in the application of NNs (especially the multiquadric (MQ) radial basis function networks (RBFNs)) for numerical solution of PDEs has been increasing (Kansa, 1990; Mai-Duy and Tran-Cong, 2001a, b, 2002; Sharan *et al.*, 1997; Zerroukat *et al.*, 1998). In this study, "universal approximator" RBFNs are introduced into the BEM scheme to represent the variables along the boundary. Although RBFNs have an ability to represent any continuous function to a prescribed degree of accuracy, practical means to acquire sufficient approximation accuracy still remain an open problem. Indirect RBFNs (IRBFNs) which perform better than direct RBFNs in terms of accuracy and convergence rate (Mai-Duy and Tran-Cong, 2001a, 2002) are utilised in this work. Due to the presence of NNs in BIs, the treatment of the singularity in CPV integrals requires some modification in comparison with the standard BEM. The paper is organised as follows. In Section 2, the IRBFN interpolation of functions is presented and its performance is then compared with linear and quadratic element results via a numerical example. Section 3 is to introduce the IRBFN interpolation into the BEM scheme to represent the variable in BIEs. In Section 4, some 2D heat transfer problems governed by Laplace's or Poisson's equations are simulated to validate the proposed method. Section 5 gives some concluding remarks.

2. Interpolation with IRBFN

The task of interpolation problems is to estimate a function $y(s)$ for arbitrary s from the known value of $y(s)$ at a set of points $s^{(1)}, s^{(2)}, \ldots, s^{(n)}$ and therefore,

the interpolation must model the function by some plausible functional form. The form is expected to be sufficiently general in order to describe large classes of functions which might arise in practice. By far the most common functional forms used are based on polynomials (Press *et al.*, 1988). Generally, for problems of interpolation, universal approximators are highly desired in order to handle large classes of functions. It has been proved that RBFNs, which can be considered as approximation schemes, are able to approximate arbitrarily well continuous functions (Girosi and Poggio, 1990). The function y to be interpolated/approximated is decomposed into radial basis functions as

$$y(x) \approx f(x) = \sum_{i=1}^{m} w^{(i)} g^{(i)}(x), \tag{1}$$

where m is the number of radial basis functions, $\{g^{(i)}\}_{i=1}^{m}$ is the set of chosen radial basis functions and $\{w^{(i)}\}_{i=1}^{m}$ is the set of weights to be found. Theoretically, the larger the number of radial basis functions used, the more accurate the approximation will be as, stated in Cover's theorem (Haykin, 1999). However, the difficulty here is how to choose the network's parameters such as RBF widths properly. IRBFNs were found to be more accurate than direct RBFNs with relatively easier choice of RBF widths (Mai-Duy and Tran-Cong, 2001a, 2002) and will be employed in the present work. In this paper, only the problems in 2D are discussed. In view of the fact that the interpolation IRBFN method will be coupled later with the BEM where the problem dimensionality is reduced by one, only the MQ-IRBFN for function and its derivatives (e.g. up to the second order) in 1D needs to be employed here and its formulation is briefly recaptured as follows:

$$y''(s) \approx f''(s) = \sum_{i=1}^{m} w^{(i)} g^{(i)}(s), \tag{2}$$

$$y'(s) \approx f'(s) = \sum_{i=1}^{m} w^{(i)} H^{(i)}(s) + C_1, \tag{3}$$

$$y(s) \approx f(s) = \sum_{i=1}^{m} w^{(i)} \bar{H}^{(i)}(s) + C_1 s + C_2, \tag{4}$$

where s is the curvilinear coordinate (arclength), C_1 and C_2 are constants of integration and

$$g^{(i)}(s) = ((s - c^{(i)})^2 + a^{(i)2})^{1/2}, \tag{5}$$

$$H^{(i)}(s) = \int g^{(i)}(s)\,\mathrm{d}s = \frac{(s-c^{(i)})((s-c^{(i)})^2 + a^{(i)2})^{1/2}}{2} + \frac{a^{(i)2}}{2}\ln((s-c^{(i)}) + ((s-c^{(i)})^2 + a^{(i)2})^{1/2}), \tag{6}$$

$$\bar{H}^{(i)}(s) = \int H^{(i)}(s)\,\mathrm{d}s = \frac{((s-c^{(i)})^2 + a^{(i)2})^{3/2}}{6} + \frac{a^{(i)2}}{2}(s-c^{(i)})\ln((s-c^{(i)}) + ((s-c^{(i)})^2 + a^{(i)2})^{1/2}) - \frac{a^{(i)2}}{2}((s-c^{(i)})^2 + a^{(i)2})^{1/2}, \tag{7}$$

in which $\{c^{(i)}\}_{i=1}^{m}$ is the set of centres and $\{a^{(i)}\}_{i=1}^{m}$ is the set of RBF widths. The RBF width is chosen based on the following simple relation

$$a^{(i)} = \beta d^{(i)},$$

where β is a factor and $d^{(i)}$ is the minimum arclength between the ith centre and its neighbouring centres. Since C_1 and C_2 are to be found, it is convenient to let $w^{(m+1)} = C_1$, $w^{(m+2)} = C_2$, $\bar{H}^{(m+1)} = s$ and $\bar{H}^{(m+2)} = 1$ in equation (4), which becomes

$$y(s) \approx f(s) = \sum_{i=1}^{m+2} w^{(i)}\bar{H}^{(i)}(s), \tag{8}$$

$$\bar{H}^{(i)} = \text{RHS of equation (7)}, \quad i = 1, \ldots, m, \tag{9}$$

$$\bar{H}^{(m+1)} = s, \tag{10}$$

$$\bar{H}^{(m+2)} = 1. \tag{11}$$

The detailed implementation and accuracy of the IRBFN method were reported previously (Mai-Duy and Tran-Cong, 2002). In all the numerical examples carried out in this paper, the value of β is simply chosen to be in the range of 7-10. Before introducing the IRBFN interpolation into the BEM scheme, the performance of the IRBFN and element-based method are compared using the interpolation of the following function

$$y = 0.02(12 + 3s - 3.5s^2 + 7.2s^3)(1 + \cos 4\pi s)(1 + 0.8 \sin 3\pi s),$$

where $0 \leq s \leq 1$ (Figure 1). The accuracy achieved by each technique is evaluated via the norm of relative error of the solution N_e defined by

$$N_e = \left(\frac{\sum_{i=1}^{q} (y(s^{(i)}) - f(s^{(i)}))^2}{\sum_{i=1}^{q} y(s^{(i)})^2} \right)^{1/2}, \quad (12)$$

where $y(s^{(i)})$ and $f(s^{(i)})$ are the exact and approximate solutions at the point i, respectively, and q is the number of test points. The performance of linear, quadratic and IRBFN interpolations are assessed using four data sets of 13, 15, 17 and 19 known points. For each data set, the function y is estimated at 500 test points. Note that the known and test points here are uniformly distributed. The results obtained using $\beta = 10$ are displayed in Figure 2 showing that the IRBFN method achieves superior accuracy and convergence rate to the element-based method. The solution converges apparently as $O(h^{1.95})$, $O(h^{1.98})$ and $O(h^{9.47})$ for linear, quadratic and IRBFN interpolations, respectively, where h is the grid point spacing. At $h = 0.06$, which corresponds to a set of 19 grid

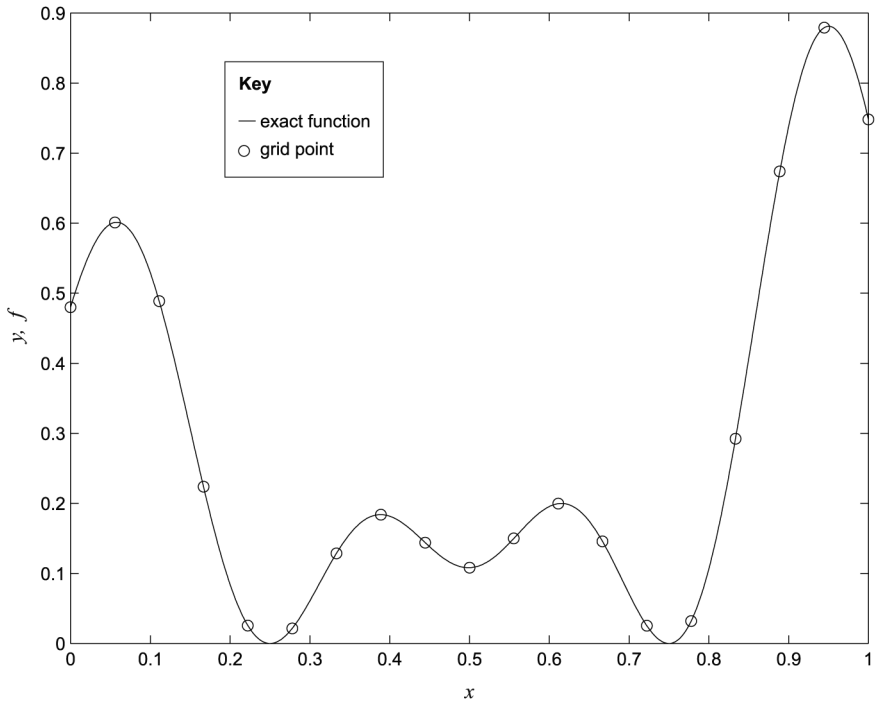

Figure 1.
Interpolation of function $y = 0.02(12 + 3x - 3.5x^2 + 7.2x^3)(1 + \cos 4\pi x)(1 + 0.8 \sin 3\pi x)$ from a set of grid points

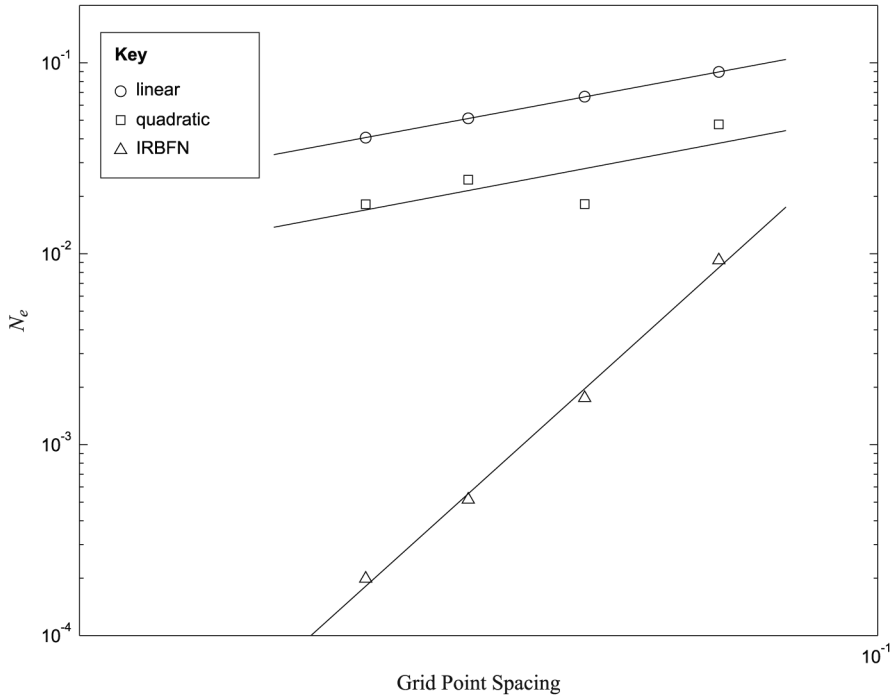

Figure 2.
Interpolation of function $y = 0.02(12 + 3x - 3.5x^2 + 7.2x^3)(1 + \cos 4\pi x)(1 + 0.8 \sin 3\pi x)$. The rate of convergence with grid point spacing refinement. The solution converges apparently as $O(h^{1.95})$, $O(h^{1.98})$ and $O(h^{9.47})$ for linear, quadratic and IRBFN interpolations, respectively, where h is the grid point spacing

points, the error norms obtained are $4.06e-2$, $1.81e-2$ and $1.98e-4$ for linear, quadratic and IRBFN schemes, respectively.

3. A new interpolation method for the evaluation of BIs

For heat transfer problems, the governing equations take the form

$$\nabla^2 u = b, \quad \mathbf{x} \in \Omega, \tag{13}$$

$$u = \bar{u}, \quad \mathbf{x} \in \Gamma_u, \tag{14}$$

$$q \equiv \frac{\partial u}{\partial n} = \bar{q}, \quad \mathbf{x} \in \Gamma_q, \tag{15}$$

where u is the temperature, q is the temperature gradient across the surface, $\mathbf{n}$ is the unit outward normal vector, $\bar{u}$ and $\bar{q}$ are the prescribed boundary conditions, b is a known function of position and $\Gamma = \Gamma_u + \Gamma_q$ is the boundary of the domain Ω.

Integral equation (IE) formulations for heat transfer problems are well documented in a number of texts (Banerjee and Butterfield, 1981; Brebbia *et al.*, 1984). Equations (13)-(15) can be reformulated in terms of the IEs for a given spatial point ξ as follows

$$c(\xi)u(\xi) + \int_{\Gamma} q^*(\xi, x)u(x)\,\mathrm{d}\Gamma + \int_{\Omega} b(x)u^*(\xi, x)\,\mathrm{d}\Omega = \int_{\Gamma} u^*(\xi, x)q(x)\,\mathrm{d}\Gamma, \quad (16)$$

where u^* is the fundamental solution to the Laplace equation, e.g. for a 2D isotropic domain $u^* = (1/2\pi)\ln(1/r)$ in which r is the distance from the point ξ to the current point of integration x, $q^* = \partial u^*/\partial n$, $c(\xi) = \theta/2\pi$ with θ being the internal angle of the corner in radians, if ξ is a boundary point and $c(\xi) = 1$, if ξ is an internal point. Note that the volume integral here does not introduce any unknowns because the function b is given and furthermore, it can be reduced to the BIs by using the particular solution (PS) techniques (Zheng *et al.*, 1991) or the dual reciprocity method (DRM) (Partridge *et al.*, 1992). Without loss of generality, the following discussions are based on equation (16) with $b = 0$ (Laplace's equation).

For the standard BEM, the numerical procedure for equation (16) involves a subdivision of the boundary Γ into a number of small elements. On each element, the geometry and the variation of u and q are assumed to have a certain shape such as linear and quadratic ones. The study on the interpolation of function in Section 2 shows that the IRBFN interpolation achieves an accuracy and convergence rate superior to the linear and quadratic element-based interpolations. The question here is whether the employment of IRBFN interpolation in the BEM scheme can improve the solution in terms of accuracy and convergence rate as in the case of function approximation. The answer is positive and substantiated in the remainder of this paper.

The first issue to be considered is about the implementation of singular integrals when IRBFNs are present within integrands. The difference between the IRBFN and the Lagrange-type interpolation is that in the present IRBFN interpolation, none of the basis functions are null at the singular point (the point_ where the field point x and the source point ξ coincide) and hence the corresponding integrands obtained are not regular. Consequently, at the singular point all CPV integrals associated with the IRBFN weights are singular and cannot be evaluated by using the hypothesis of constant potential directly over the whole domain as in the case of the standard BEM. To overcome this difficulty, the treatment of singular CPV integrals needs to be slightly modified. The BIEs can be written in the following form (Hwang *et al.*, 2002; Tanaka *et al.*, 1994)

$$u(\xi)\int_{\Gamma_\varepsilon, \varepsilon \to 0} q^*(\xi, x)\,\mathrm{d}\Gamma + \mathrm{CPV}\int_{\Gamma} q^*(\xi, x)u(x)\,\mathrm{d}\Gamma = \int_{\Gamma} u^*(\xi, x)q(x)\,\mathrm{d}\Gamma, \quad (17)$$

where Γ_ε is part of a circle that excludes its origin (or the singular point) from the domain of analysis. Assume that the temperature $u(x)$ is a constant unit on

the whole domain, i.e. $u(\xi) = u(x) = 1$, and hence the gradient $q(x)$ is everywhere zero. Equation (17) then simplifies to

$$\int_{\Gamma_\varepsilon, \varepsilon \to 0} q^*(\xi, x)\, \mathrm{d}\Gamma = -\mathrm{CPV} \int_\Gamma q^*(\xi, x)\, \mathrm{d}\Gamma. \tag{18}$$

Substitution of equation (18) into equation (17) yields

$$\mathrm{CPV} \int_\Gamma q^*(\xi, x)(u(x) - u(\xi))\, \mathrm{d}\Gamma = \int_\Gamma u^*(\xi, x) q(x)\, \mathrm{d}\Gamma. \tag{19}$$

The CPV integral is now written in the non-singular form, where the standard Gaussian quadrature can be applied. For weakly singular integrals, some well-known treatments such as logarithmic Gaussian quadrature and Telles' transformation technique (Telles, 1987) can be applied directly as in the case of the standard BEM.

The second issue is concerned with the employment of the IRBFNs in the BEM scheme to represent the variables in the BIs. In the present method, the boundary Γ of the domain of analysis is also divided into a number of segments N_s, i.e.

$$\Gamma = \sum_{j=1}^{N_s} \Gamma_j,$$

which are 1D domains to be represented by networks. Note that the size of the segment Γ_j can be much larger than the size of elements in the standard BEM provided that the associated boundary is smooth and the prescribed boundary conditions are of the same type. Equation (19) can be written in the discretised form as

$$\sum_{j=1}^{N_s} \int_{\Gamma_j} q^*(\xi, x)(u_j(x) - u_l(\xi))\, \mathrm{d}\Gamma_j = \sum_{j=1}^{N_s} \int_{\Gamma_j} u^*(\xi, x) q_j(x)\, \mathrm{d}\Gamma_j, \tag{20}$$

where the subscript j denotes the general segments and the subscript l indicates the segment containing the source point ξ. The variation of temperature u and gradient q on the segment Γ_j is now represented by the IRBFNs in terms of the curvilinear coordinate s as (equation (9))

$$u_j = \sum_{i=1}^{mj+2} w_{uj}^{(i)} \bar{H}_j^{(i)}(s), \tag{21}$$

$$q_j = \sum_{i=1}^{mj+2} w_{qj}^{(i)} \bar{H}_j^{(i)}(s), \tag{22}$$

where $s \in \Gamma_j$, $mj+2$ is the number of IRBFN weights, $\{w_{uj}^{(i)}\}_{i=1}^{mj+2}$ and $\{w_{qj}^{(i)}\}_{i=1}^{mj+2}$ are the sets of weights of networks for the temperature u and temperature gradient q, respectively. Similarly, the geometry can be interpolated from the nodal value by using the IRBFNs as

$$x_{1j} = \sum_{i=1}^{mj+2} w_{x1j}^{(i)} \bar{H}_j^{(i)}(s), \tag{23}$$

$$x_{2j} = \sum_{i=1}^{mj+2} w_{x2j}^{(i)} \bar{H}_j^{(i)}(s). \tag{24}$$

Substitution of equations (21) and (22) into equation (20) yields

$$\begin{aligned} &\sum_{j=1}^{N_s} \int_{\Gamma_j} q^*(\xi, s) \left(\sum_{i=1}^{mj+2} w_{uj}^{(i)} \bar{H}_j^{(i)}(s) - \sum_{i=1}^{ml+2} w_{ul}^{(i)} \bar{H}_l^{(i)}(\xi) \right) \mathrm{d}\Gamma_j \\ &\quad = \sum_{j=1}^{N_s} \int_{\Gamma_j} u^*(\xi, s) \left(\sum_{i=1}^{mj+2} w_{qj}^{(i)} \bar{H}_j^{(i)}(s) \right) \mathrm{d}\Gamma_j, \end{aligned} \tag{25}$$

or,

$$\begin{aligned} &\sum_{j=1}^{N_s} \left\{ \sum_{i=1}^{mj+2} w_{uj}^{(i)} \left(\int_{\Gamma_j} q^*(\xi, s) \bar{H}_j^{(i)}(s)\, \mathrm{d}\Gamma_j \right) - \sum_{i=1}^{ml+2} w_{ul}^{(i)} \left(\int_{\Gamma_j} q^*(\xi, s) \bar{H}_l^{(i)}(s)\, \mathrm{d}\Gamma_j \right) \right\} \\ &\quad = \sum_{j=1}^{N_s} \sum_{i=1}^{mj+2} w_{qj}^{(i)} \left(\int_{\Gamma_j} u^*(\xi, s) \bar{H}_j^{(i)}(s)\, \mathrm{d}\Gamma_j \right), \end{aligned} \tag{26}$$

where mj is the number of training points on the segment j, which can vary from segment to segment. Equation (26) is formulated in terms of the IRBFN weights of networks for u and q rather than the nodal values of u and q as in the case of the standard BEM. Locating the source point ξ at the boundary training points results in the underdetermined system of algebraic equations with the unknown being the IRBFN weights. Thus, the system of equations obtained, which can have many solutions, needs to be solved in the general least squares sense. The preferred solution is the one whose values are smallest in the least squares sense (i.e. the norm of components is minimum). This can be achieved by using singular value decomposition technique (SVD). The procedural flow chart can be briefly summarised as follows:

(1) divide the boundary into a number of segments over each of which the boundary is smooth and the prescribed boundary conditions are of the same type;

(2) apply the IRBFN for approximation of the prescribed physical boundary conditions in order to obtain the IRBFN weights which are the boundary conditions in the weight space;

(3) form the system matrices associated with the IRBFN weights w_u and w_q;

(4) impose the boundary conditions obtained from the step 2 and then solve the system for IRBFN weights by the SVD technique;

(5) compute the boundary solution by using the IRBFN interpolation;

(6) evaluate the temperature and its derivatives at selected internal points;

(7) output the results.

Note that for the numerical solution of Poisson's equations using the BEM-PS approach, the PS is first found by expressing the known function b as a linear combination of radial basis functions and the volume integral is then transformed into the BIs (Zheng *et al.*, 1991). However, the first stage of this process produces a certain error which is separate from the error in the evaluation of the BIs. In order to confine the error of solution only to the evaluation of BIs, the following numerical examples of heat transfer problems governed by the Laplace's equations or Poisson's equations are chosen where the associated analytical PSs exist for the latter.

4. Numerical examples

In this section, the proposed method is verified and compared with the standard BEM on heat transfer problems governed by the Laplace's or Poisson's equations. In order to make the BEM programs general in the sense that they can deal with any types of boundary conditions at the corners, all BEM codes with linear, quadratic and IRBFN interpolations employ discontinuous elements at the corner. The extreme boundary point at the corner is shifted into the element by one-fourth of the length of the element. Integrals are evaluated by using the standard Gaussian quadrature for regular cases and logarithmic Gaussian quadrature or Telles' quadratic transformation (Telles, 1987) for weakly singular cases with nine integration points. For the purpose of error estimation and convergence study, the error norm defined in equation (12) will be utilised here with the function y being the temperature u and its normal derivative q in the case of the boundary solution or the temperature u in the case of the internal solution.

4.1 Boundary geometry with straight lines

It can be seen that the linear interpolation is able to represent exactly the geometry for a straight line and hence on the straight line segment the IRBFN

interpolation needs only to be used for representing the variation of temperature and gradient.

4.1.1 Example 1. Consider a square closed domain whose dimensions are taken to be 6 by 6 units as shown in Figure 3. The temperature on the left and right edges is maintained at 300 and 0, respectively, while the homogeneous Neumann conditions $q = 0$ are imposed on the other edges. Inside the square, the steady-state temperature satisfies the Laplace's equation. The analytical solution is

$$u(x_1, x_2) = 300 - 50x_1.$$

This is a simple problem where the variation of temperature is linear. It can be seen that the use of linear interpolation is the best choice for this problem. Both linear and IRBFN ($\beta = 10$) interpolations are employed and the corresponding BEM results on the boundary and at some internal points are displayed in Table I showing that the proposed method as well as the linear-BEM works. Significantly, the IRBFN-BEM works increasingly better than the linear-BEM as the number of boundary points increases, which seems to indicate that the IRBFN-BEM does not suffer numerical ill-conditioning as in the case of the standard BEM. Note that in the case of the IRBFN interpolation, each edge of the square domain and the boundary points on it become the domain and training points of the network associated with the edge, respectively. It is expected that the IRBFN-BEM approach performs better in dealing with higher order variations of temperature, which is verified in the following examples.

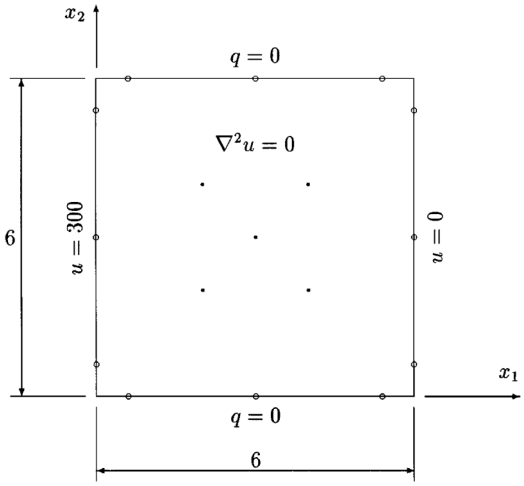

Figure 3.
Example 1 – geometry, boundary conditions, boundary points and internal points

4.1.2 Example 2. The problem is to find the temperature field such that

$$\nabla^2 u = 0 \quad \text{inside the square } 0 \le x_1 \le \pi,\ 0 \le x_2 \le \pi, \tag{27}$$

$$u(x_1, \pi) = \sin(x_1) \quad \text{on the top edge } (0 \le x_1 \le \pi), \tag{28}$$

$$u(x_1, x_2) = 0 \quad \text{on the other three sides.} \tag{29}$$

The exact solution of this problem is given by Snider (1999)

$$u(x_1, x_2) = \frac{1}{\sinh(\pi)} \sin(x_1) \sinh(x_2).$$

This is a Dirichlet problem for which the essential boundary condition is imposed along the boundary. Using discontinuous boundary elements at the corner for the case of the standard BEM or shifting the training points at the corner into the adjacent segments for the case of the IRBFN-BEM allows the correct description of multi-valued gradient q at the corner. In the case of IRBFN interpolation, each side of the square domain becomes the domain of network and the boundary points on it are utilised as training points. To study the convergence of the present method, four boundary point densities, namely $5 \times 4, 7 \times 4, 9 \times 4$ and 11×4, and $\beta = 7$ are employed. Some internal points are selected at $(\pi/3, \pi/3)$, $(\pi/3, 2\pi/3)$, $(\pi/2, \pi/2)$, $(2\pi/3, \pi/3)$ and $(2\pi/3, 2\pi/3)$. The performance of the BEM with linear, quadratic and IRBFN interpolations is assessed using the error norms of the boundary and internal solution. The boundary solution is displayed in Figure 4 showing that the proposed method is the most accurate one with higher convergence rate achieved. With these given boundary point densities, the solution converges as $O(h^{2.24})$, $O(h^{2.04})$ and $O(h^{3.83})$ for linear, quadratic and IRBFN interpolations, respectively. At $h = 0.31$, which corresponds to the boundary point density of 11×4, error norms obtained are $1.27e-2$, $1.17e-2$

Boundary points	3×4	4×4	5×4	6×4
Linear elements	8	12	16	20
Error norm of the boundary solution				
Linear-BEM	$3.01e-7$	$3.08e-7$	$3.72e-7$	$4.30e-7$
IRBFN-BEM	$7.22e-6$	$1.17e-6$	$4.33e-7$	$1.60e-7$
Error norm of the internal solution				
Linear-BEM	$1.86e-7$	$1.43e-7$	$1.22e-7$	$1.07e-7$
IRBFN-BEM	$3.97e-6$	$4.07e-7$	$1.57e-7$	$5.17e-8$

Note: The selected internal points are (2, 2), (2, 4), (3, 3), (4, 2) and (4, 4). In the first row, $n \times m$ means n boundary points per segment and m segments. The number of boundary elements in each case results in the same total number of boundary points

Table I.
Example 1 – error norms N_es of the IRBFN-BEM and linear-BEM solutions

and $2.80e-5$ for linear, quadratic and IRBFN interpolations, respectively. The internal results are recorded in Table II showing that the IRBFN-BEM achieves a solution accuracy better than the linear/quadratic-BEM results by several orders of magnitude.

4.1.3 Example 3. The problem is to find the temperature field such that

$$\nabla^2 u = 0 \quad \text{inside the square } 0 \le x_1 \le \pi, 0 \le x_2 \le \pi, \tag{30}$$

$$u(\pi, x_2) = \sin^3(x_2) \quad \text{on the right edge } (0 \le x_2 \le \pi), \tag{31}$$

$$u(x_1, x_2) = 0 \quad \text{on the other three sides.} \tag{32}$$

The analytical solution of this problem (Snider, 1999) is

$$u(x_1, x_2) = \frac{3}{4\sinh(\pi)}\sin(x_2)\sinh(x_1) - \frac{1}{4\sinh(3\pi)}\sin(3x_2)\sinh(3x_1).$$

The shape of this solution is more complicated than the one in the previous example and provides a good test for the present method. The boundary point

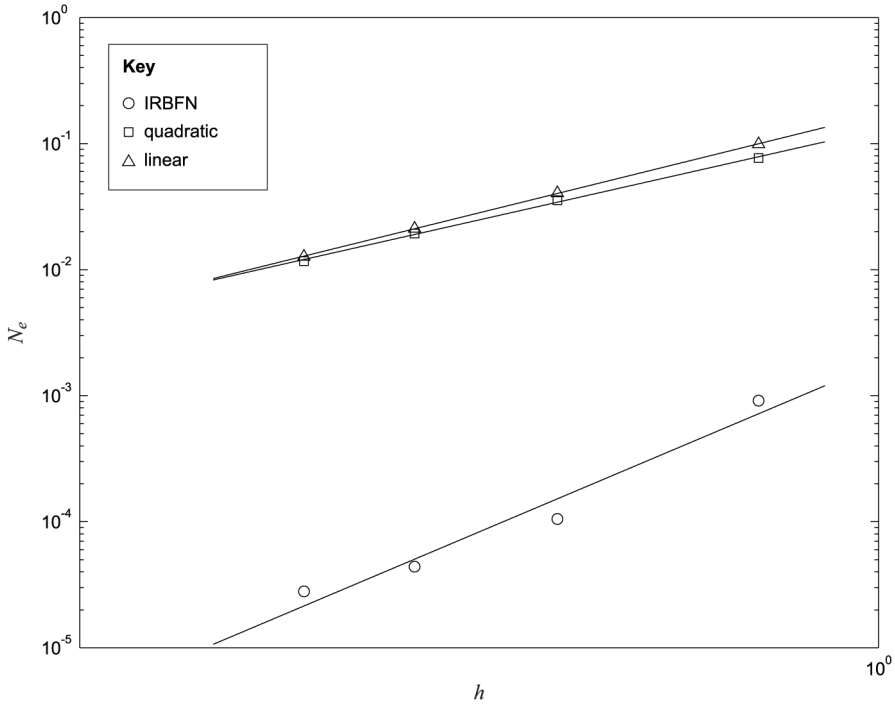

Note: With the given boundary point densities of 5×4, 7×4, 9×4 and 11×4, the rate of convergence appears to be $O(h^{2.24})$, $O(h^{2.04})$ and $O(h^{3.83})$ for linear, quadratic and IRBFN interpolations, respectively, as depicted by solid lines. The proposed method achieves accuracy and convergence rate superior to the element-based method

Figure 4.
Example 2 – error norm N_e of the boundary solution versus boundary point spacing h obtained by the BEM with different interpolation techniques

densities are chosen to be 9×4, 11×4, 13×4 and 15×4. The selected internal points are $(\pi/3, \pi/3)$, $(\pi/3, 2\pi/3)$, $(\pi/2, \pi/2)$, $(2\pi/3, \pi/3)$ and $(2\pi/3, 2\pi/3)$. The proposed method also performs much better than the standard BEM and similar remarks as mentioned in Example 2 apply. With $\beta = 7$, the error norms of the boundary solution and the internal solution are displayed in Figure 5 and Table III, respectively. The rates of convergence of the boundary solution are of $O(h^{2.14})$, $O(h^{1.38})$ and $O(h^{4.78})$ for linear, quadratic and IRBFN interpolations,

Table II.
Example 2 – error norms N_es of the internal solution obtained by the BEM with different interpolation techniques

Boundary points	5×4	7×4	9×4	11×4
Linear	$2.96e-2$	$1.25e-2$	$6.90e-3$	$4.30e-3$
Quadratic	$2.80e-3$	$5.90e-4$	$1.82e-4$	$7.66e-5$
IRBFN	$1.27e-5$	$4.79e-7$	$1.49e-7$	$3.40e-8$

Note: The IRBFN-BEM yields a solution more accurate than the linear/ quadratic-BEM by several orders of magnitude

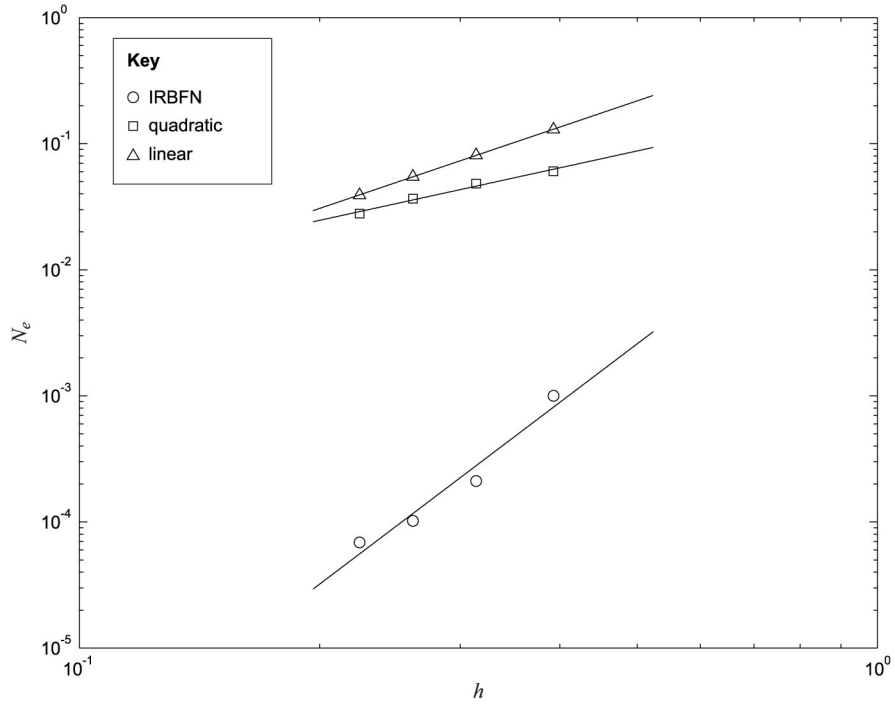

Figure 5.
Example 3 – error norm N_e of the boundary solution versus boundary point spacing h obtained from the BEM with different interpolation techniques

Note: With the given boundary point densities of 9×4, 11×4, 13×4 and 15×4, the rate of convergence appears to be $O(h^{2.14})$, $O(h^{1.38})$ and $O(h^{4.78})$ for linear, quadratic and IRBFN interpolations, respectively, as depicted by solid lines. The proposed method achieves accuracy and convergence rate superior to the element-based method

respectively. At $h = 0.07$, which corresponds to the boundary point density of 15×4, the achieved error norms are $3.91e-2$, $2.79e-2$ and $6.88e-5$ for linear, quadratic and IRBFN interpolations, respectively. The accuracy of the internal solution by the present method is also better, by several orders of magnitude, than the ones by linear and quadratic BEMs. Furthermore, the CPU time requirements for the two methods are compared in Table IV. The structures of the MATLAB codes are the same and therefore it is believed that the higher efficiency achieved by the IRBFN-BEM is due to the fact that the number of segments (elements) used in the IRBFN-BEM is significantly less than that used in the standard BEM, resulting in a better vectorised computation for the former (MATLAB's internal vectorisation).

4.2 Boundary geometry with curved and straight segments

NNs are employed to interpolate not only the variables u and q by using equations (21) and (22), but also the geometry of the curved segments by using equations (23) and (24). All quantities in the BIs such as u, q and $d\Gamma$ are represented by IRBFNs necessarily in terms of the curvilinear coordinate (arclength) s. Special attention is given to the transformation of the quantity $d\Gamma$ from rectangular to curvilinear coordinates where the use of a Jacobian is required as follows

$$d\Gamma = \left(\left(\frac{\partial x_1}{\partial s} \right)^2 + \left(\frac{\partial x_2}{\partial s} \right)^2 \right)^{1/2} ds, \tag{33}$$

in which the derivatives of x_1 and x_2 on the segment Γ_j can be expressed in terms of the basis function H (equation (6)) as

Boundary points	9×4	11×4	13×4	15×4
Linear	$6.60e-3$	$4.20e-3$	$2.90e-3$	$2.20e-3$
Quadratic	$3.25e-4$	$1.74e-4$	$7.84e-5$	$4.09e-5$
IRBFN	$2.79e-6$	$1.91e-6$	$7.97e-7$	$9.64e-7$

Note: The IRBFN-BEM yields a solution more accurate than the linear/quadratic-BEM by several orders of magnitude

Table III. Example 3 – error norms N_es of the internal solution obtained by the BEM with different interpolation techniques

	Linear-BEM		IRBFN-BEM	
Mesh	Boundary solution	Total solution	Boundary solution	Total solution
9×9	1.98	4.57	2.07	2.19
11×11	3.02	8.39	3.08	3.27
13×13	4.29	13.88	4.27	4.63
15×15	5.78	21.56	5.70	6.33

Note: The code is written in the MATLAB language (version R11.1 by The MathWorks, Inc.), which is run on a 548 MHz Pentium PC. Note that MATLAB language is interpretative

Table IV. Example 3 – CPU times (s) used to obtain the boundary solution and the total solution by the linear-BEM and IRBFN-BEM

$$\frac{\partial x_{1j}}{\partial s} = \sum_{i=1}^{mj+2} w_{x1j}^{(i)} H_j^{(i)}(s), \tag{34}$$

$$\frac{\partial x_{2j}}{\partial s} = \sum_{i=1}^{mj+2} w_{x2j}^{(i)} H_j^{(i)}(s). \tag{35}$$

Clearly, these derivatives can be calculated straightforwardly, once the interpolation of the function is done after solving equations (23) and (24). For more details covering the calculation of derivative functions by IRBFNs, the reader is referred to Mai-Duy and Tran-Cong (2002). Normally, the orders of IRBFN approximation for the boundary geometry and the variation of u and q are chosen to be the same. However, they can be different and are discussed shortly.

4.2.1 Example 4. Consider the boundary value problem governed by the Laplace equation

$$\nabla^2 u = 0$$

as shown in Figure 6. The domain of analysis is one quarter of the ellipse and the boundary conditions are

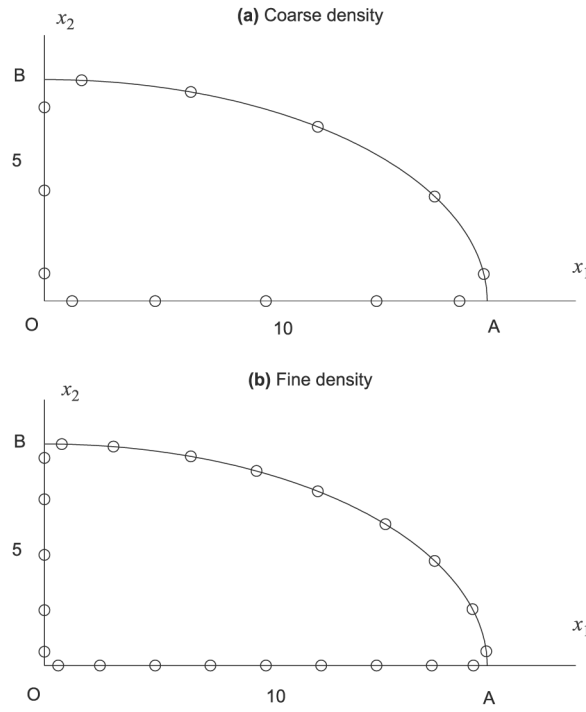

Figure 6.
Example 4 – geometry definition and training points

$$u = 0,$$

on OA and BO and

$$\frac{\partial u}{\partial n} = -\frac{a^2 - b^2}{(a^4 x_2^2 + b^4 x_1^2)^{1/2}} x_1 x_2,$$

on AB with a and b being the half lengths of the major and minor axes, respectively. This problem with $a = 10$ and $b = 5$ was solved by quadratic BEM (Brebbia and Dominguez, 1992) using five and ten quadratic elements with two selected internal points (2, 2) and (4, 3.5). For the present method, the boundary is divided into three segments (two straight lines and one curve) and the training points are taken to be the same as the boundary nodes used in the case of the quadratic BEM. Thus, the densities are 5, 5 and 3 on segments OA, AB and BO, respectively, which corresponds to the case of five quadratic elements and densities 9, 9 and 5 corresponding to the case of ten quadratic elements. In order to compare the present results with the results obtained by quadratic BEM (Brebbia and Dominguez, 1992) and the exact solution, some values of the function u are extracted and the errors obtained by the two methods are displayed in Tables V and VI, which show that the present method yields better accuracy. For example, with four digit scaled fixed point, for the coarse density the range of the error is (0.02-0.2 per cent) and (0.84-2.32 per cent) for IRBFN-BEM and quadratic BEM, respectively, while for the fine density the error range is (0.00-0.02 per cent) and (0.02-0.14 per cent) for IRBFN-BEM and quadratic BEM, respectively.

4.2.2 Example 5. The distribution of the function u in an ellipse with a semi-major axis $a = 2$ and a semi-minor axis $b = 1$ is described by

$$\nabla^2 u = -2, \tag{36}$$

subject to the condition $u = 0$ along the boundary Γ. The exact solution is

$$u(x_1, x_2) = -0.8\left(\frac{x_1^2}{a^2} + \frac{x_2^2}{b^2} - 1\right).$$

		Exact	IRBFN-BEM		Quadratic BEM	
x_1	x_2	u	u	Error (per cent)	u	Error (per cent)
8.814	2.362	−12.489	−12.514	0.20	−12.779	2.32
6.174	3.933	−14.570	−14.579	0.06	−14.839	1.85
3.304	4.719	−9.356	−9.354	0.02	−9.435	0.84
2.000	2.000	−2.400	−2.404	0.17	−2.431	1.29
4.000	3.500	−8.400	−8.413	0.15	−8.472	0.86

Note: Comparison of the error obtained by the present IRBFN-BEM ($\beta = 7$) and the quadratic BEM using the same boundary nodes (five quadratic elements)

Table V.
Example 4 – comparison (five quadratic elements)

This problem is governed by the Poisson's equation and hence the BEM with PS can be applied here for obtaining the numerical solution. The solution u can be decomposed into a homogeneous part u^{H} and a PS part u^{P} as

$$u = u^{\mathrm{H}} + u^{\mathrm{P}}.$$

The PS to equation (36) can be verified to be

$$u^{\mathrm{P}} = -\frac{x_1^2 + x_2^2}{2}$$

while the complementary one satisfies the Laplace's equation $\nabla^2 u^{\mathrm{H}} = 0$ with the boundary condition $u^{\mathrm{H}} = -u^{\mathrm{P}}$ on Γ. The latter is to be solved by BEM. Partridge *et al.* (1992) used this approach to solve the problem in which 16 linear boundary elements are employed and the solution obtained was displayed at seven internal points. In the present method, the boundary Γ is divided into two segments as shown in Figure 7. Four data densities, namely 9×2, 11×2, 13×2 and 15×2, and $\beta = 8$ are employed to simulate the problem. Error norms of the boundary solution obtained are 0.0105, 0.0037, $9.4436e-4$ and $5.8135e-4$ for the four densities, respectively, with the convergence rate achieved being $O(N^{(-5.9289)})$, where N is the number of the training boundary points employed (Figure 8). In order to compare with the linear BEM (Partridge *et al.*, 1992), the solution at seven internal points is also computed by the present method and the corresponding error norms obtained are 0.0063, 0.0026, $8.0387e-4$ and $3.4900e-5$ for the four densities, respectively. Hence with the coarse density of 9×2 that corresponds to 16 linear boundary elements, the present method achieves the error norm of 0.0063, while the linear BEM achieves only $N_{\mathrm{e}} = 0.0109$. The latter number is calculated by the present authors using the table shown in Partridge *et al.* (1992). Numerical result for the finest density is displayed in Table VII.

4.2.3 Interpolation for geometry and boundary variables. In the last two examples, the IRBFN interpolations for the geometry and the variables u and q

		Exact	IRBFN-BEM		Quadratic BEM	
x_1	x_2	u	u	Error (per cent)	u	Error (per cent)
8.814	2.362	−12.489	−12.487	0.02	−12.506	0.14
6.174	3.933	−14.570	−14.568	0.01	−14.576	0.04
3.304	4.719	−9.356	−9.355	0.01	−9.363	0.07
2.000	2.000	−2.400	−2.400	0.00	−2.399	0.04
4.000	3.500	−8.400	−8.400	0.00	−8.402	0.02

Table VI.
Example 4 – comparison (ten quadratic elements)

Note: Comparison of the error obtained by the present IRBFN-BEM ($\beta = 7$) and the quadratic BEM using the same boundary nodes (ten quadratic elements)

have the same order, i.e. the training points used are same for both the cases. However, the order of IRBFN interpolation can be chosen differently for the geometry and the variables u and q in order to obtain high quality solutions with low cost as possible. The geometry is usually known and hence the

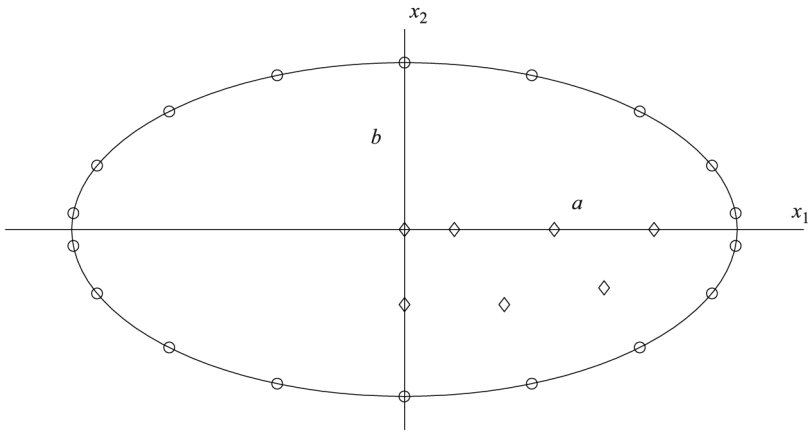

Figure 7.
Example 5 – geometry definition, boundary training points and internal points. The boundary is divided into two segments ($-a \leq x_1 \leq a$, $x_2 \geq 0$) and ($-a \leq x_1 \leq a$, $x_2 \leq 0$)

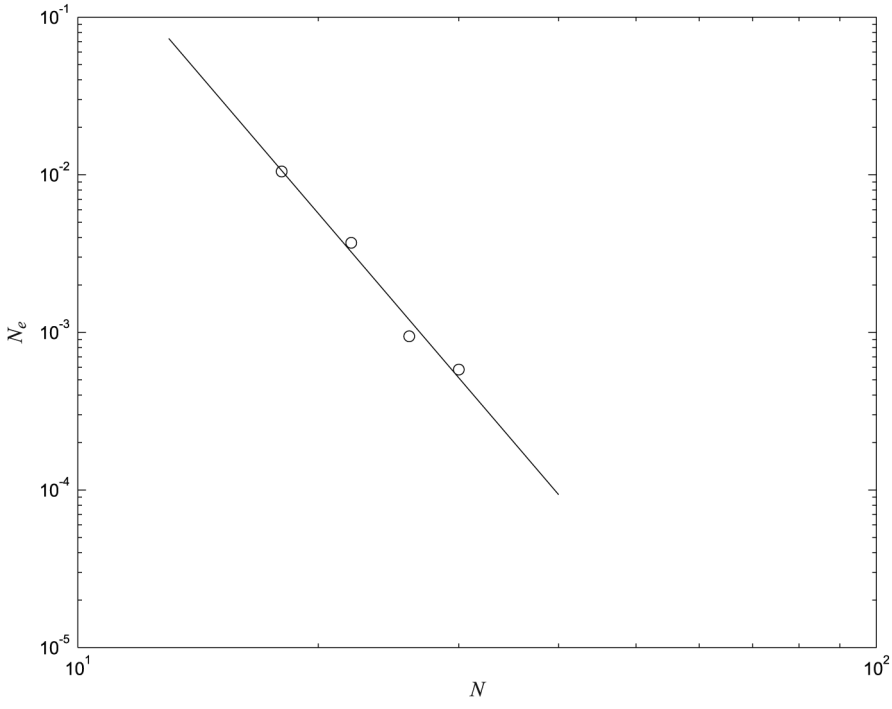

Figure 8.
Example 5 – error norm N_e of the boundary solution versus the number of boundary points N by the present IRBFN-BEM. With the given boundary point densities of 9×2, 11×2, 13×2 and 15×2, the rate of convergence appears as $O(N^{-5.9289})$, where N is the number of the boundary points employed

number of training points for the geometry interpolation can be estimated. It is emphasised that the size of the final system of equations only depends on the order of IRBFN interpolation for the variables u and q and hence in the case of highly curved boundary, it is recommended that the order of IRBFN interpolation can be chosen higher for the geometry than for the variables u and q. The problem in the last example is solved again with the increasing number of training points for the geometry interpolation. The density of training points employed is 9×2 for the variables u and q while they are 12×2 and 14×2 for the geometry. The solution is improved as shown in Table VIII. For example, the error norm of the boundary solution decreases from 0.0105 for the normal case (the same order) to $9.5093e-4$ and $8.2902e-4$ for the increasing order of geometry interpolation.

5. Concluding remarks

In this paper, the introduction of IRBFN interpolation into the BEM scheme to represent the variables in BIEs for numerical solution of heat transfer problems is implemented and verified successfully. Numerical examples show that the proposed method considerably improves the estimate of the BIs resulting in

Table VII.
Example 5 – the boundary solution obtained by the present IRBFN-BEM using the density of 15×2

Coordinates		Exact	Computed
x_1	x_2	Gradient q	Gradient q
1.997	0.056	−0.804	−0.802
1.950	0.223	−0.857	−0.859
1.802	0.434	−1.001	−1.000
1.564	0.623	−1.177	−1.178
1.247	0.782	−1.347	−1.347
0.868	0.901	−1.483	−1.483
0.445	0.975	−1.570	−1.570
0.000	1.000	−1.600	−1.600

Note: Although no symmetry condition was imposed in the numerical model, the results obtained are accurately symmetrical. Owing to symmetry, the displayed results corresponds to only a quarter of the elliptical domain

Table VIII.
Example 5 – error norms obtained by the present method with increasing order of the IRBFN interpolation for the geometry

N_e	9×2	12×2	14×2
Boundary solution	0.0105	$9.5093e-4$	$8.2902e-4$
Internal solution	0.0063	$1.5961e-4$	$9.8966e-5$

Note: The densities of IRBFN interpolation are 9×2 for the boundary variables and 9×2, 12×2 and 14×2 for the geometry

better solutions not only in terms of the accuracy but also in terms of the rate of convergence. The CPV integral is written in the non-singular form where the standard Gaussian quadrature can be applied while the weakly singular integrals are evaluated by using the well-known numerical techniques as in the case of the standard BEM. The method can be extended to problems of viscous flows which will be carried out in future work.

References

Banerjee, P.K. and Butterfield, R. (1981), *Boundary Element Methods in Engineering Science*, McGraw-Hill, London.

Brebbia, C.A. and Dominguez, J. (1992), *Boundary Elements: An Introductory Course*, Computational Mechanics Publications, Southampton.

Brebbia, C.A., Telles, J.C.F. and Wrobel, L.C. (1984), *Boundary Element Techniques: Theory and Applications in Engineering*, Springer-Verlag, Berlin.

Cybenko, G. (1989), "Approximation by superpositions of sigmoidal functions", *Mathematics of Control Signals and Systems*, Vol. 2, pp. 303-14.

Girosi, F. and Poggio, T. (1990), "Networks and the best approximation property", *Biological Cybernetics*, Vol. 63, pp. 169-76.

Haykin, S. (1999), *Neural Networks: A Comprehensive Foundation*, Prentice-Hall, NJ.

Hwang, W.S., Hung, L.P. and Ko, C.H. (2002), "Non-singular boundary integral formulations for plane interior potential problems", *International Journal for Numerical Methods in Engineering*, Vol. 53 No. 7, pp. 1751-62.

Kansa, E.J. (1990), "Multiquadrics – a scattered data approximation scheme with applications to computational fluid-dynamics – II. Solutions to parabolic, hyperbolic and elliptic partial differential equations", *Computers and Mathematics with Applications*, Vol. 19 Nos 8/9, pp. 147-61.

Mai-Duy, N. and Tran-Cong, T. (2001a), "Numerical solution of differential equations using multiquadric radial basis function networks", *Neural Networks*, Vol. 14 No. 2, pp. 185-99.

Mai-Duy, N. and Tran-Cong, T. (2001b), "Numerical solution of Navier-Stokes equations using multiquadric radial basis function networks", *International Journal for Numerical Methods in Fluids*, Vol. 37, pp. 65-86.

Mai-Duy, N. and Tran-Cong, T. (2002), "Mesh-free radial basis function network methods with domain decomposition for approximation of functions and numerical solution of Poisson's equations", *Engineering Analysis with Boundary Elements*, Vol. 26 No. 2, pp. 133-56.

Partridge, P.W., Brebbia, C.A. and Wrobel, L.C. (1992), *The Dual Reciprocity Boundary Element Method*, Computational Mechanics Publications, Southampton.

Press, W.H., Flannery, B.P., Teukolsky, S.A. and Vetterling, W.T. (1988), *Numerical Recipes in C: The Art of Scientific Computing*, Cambridge University Press, Cambridge.

Sharan, M., Kansa, E.J. and Gupta, S. (1997), "Application of the multiquadric method for numerical solution of elliptic partial differential equations", *Journal of Applied Science and Computation*, Vol. 84, pp. 275-302.

Sladek, V. and Sladek, J. (1998), *Singular Integrals in Boundary Element Methods*, Computational Mechanics Publications, Southampton.

Snider, A.D. (1999), *Partial Differential Equations: Sources and Solutions*, Prentice-Hall, NJ.

Tanaka, M., Sladek, V. and Sladek, J. (1994), "Regularization techniques applied to boundary element methods", *Applied Mechanics Reviews*, Vol. 47, pp. 457-99.

Telles, J.C.F. (1987), "A self-adaptive co-ordinate transformation for efficient numerical evaluation of general boundary element integrals", *International Journal for Numerical Methods in Engineering*, Vol. 24, pp. 959-73.

Zerroukat, M., Power, H. and Chen, C.S. (1998), "A numerical method for heat transfer problems using collocation and radial basis functions", *International Journal for Numerical Methods in Engineering*, Vol. 42, pp. 1263-78.

Zheng, R., Coleman, C.J. and Phan-Thien, N. (1991), "A boundary element approach for non-homogeneous potential problems", *Computational Mechanics*, Vol. 7, pp. 279-88.